

## SYNCHRONISATION EFFECTS AND CHAOS IN THE VAN DER POL-MATHIEU OSCILLATOR

JERZY WARMIŃSKI

*Department of Applied Mechanics, Technical University of Lublin*

*e-mail: jwar@archimedes.pol.lublin.pl*

Analysis of a nonlinear oscillator system with one degree of freedom, which includes the van der Pol self-excitation term and parametric excitation of the Mathieu type is carried out in this paper. Interactions between the parametric and self-excited vibrations for regular and chaotic motion are investigated. Synchronisation areas near the main parametric resonance and transition conditions from regular to chaotic motion are determined in this paper. It is also presented that a small external force causes qualitative and quantitative changes in the main parametric resonance and that the external harmonic force transits the system from chaos to regular motion.

*Key words:* vibration, self- and parametric excitation, synchronisation, chaos

### 1. Introduction

Self-excited vibrations can occur in many mechanical systems, for example in journal bearings lubricated with a thin oil film, flutter of a plane wing, shimmy of vehicle wheels, chatter vibrations during machine cutting. To describe self-excitation, in engineer practice, different types of models are applied. Self-excited vibrations of mechanical systems are often modelled by Rayleigh's function, which depends only on velocity of the system  $(-\alpha + \beta x'^2)x'$ , however more popular is van der Pol's model (Hayashi, 1964; Tondl, 1978; Awrejcewicz, 1990; Kapitaniak and Steeb, 1991), which depends on the velocity and square of the generalised coordinate  $(-\alpha + \beta x^2)x'$ .

In literature lots of papers are devoted to interactions of self-excited systems with other types of excitation. The interactions between two different types of vibrations can lead to very interesting phenomena. One of the first

very important works concerned with a self-excited system and external excitation, was presented in the monograph by Hayashi (1964). Analysis of the interactions of the van der Pol oscillator with a harmonic external force was carried out in that monograph. An analytical averaging method and analogue simulation results, for regular vibrations around harmonic, subharmonic and superharmonic resonance regions were there presented. Synchronisation phenomena depending on pulling in the self-excited vibration frequency by the external force and quasi-periodic limit cycles were observed on the special Hayashi plane. In the last years analysis of the van der Pol-Duffing oscillator forced by external inertial and static forces was presented by Awrejcewicz (1990, 1996). Analysis of characteristic multipliers demonstrated that for system two types of transition from regular to chaotic motion were possible: hard – when one of the multipliers is  $+1$ , and soft – after a cascade of period doubling bifurcations. Analysis of self- and external excited system with many degree-of-freedom, and their transition to chaotic and hyperchaotic motions were presented by Kapitaniak and Steeb (1991). Litak et al. (1999) investigated the interactions in Froude's pendulum forced externally as well. By applying the method of multiple scale of time, regular vibrations near the fundamental external resonance were determined. To find the critical value of the external force, which transits the system to chaos, Melnikov's criterion was applied. Examples self-excited systems forced externally can be found in the works by Guckenheimer and Holmes (1997), Steeb and Kunick (1987).

Parametric and self-excited vibrations belong to another class of very important dynamical systems. The main difference, when compared with externally forced systems, is that their vibration generally results from periodically changing stiffness or mass moment of inertia. For example one can observe such vibrations in shafts whose bending stiffness changes periodically during rotation, crank shafts with variable mass moment of inertia of the whole crank-piston system, in a wheel of a car with periodically changing radial rigidity of the tyre or in toothed gear systems where the meshing stiffness changes periodically. Hill's equation or, in a particular case, Mathieu's equation often approximate this kind of vibration.

Parametric and self-excited vibrations of the van der Pol-Mathieu oscillator for different nonlinearities were thoroughly analysed by Tondl (1978). For this class of oscillators, the synchronisation phenomenon appeared near parametric resonances regions. The amplitude of the synchronised vibrations was determined near the parametric resonances and a new method to describe quasi-periodic limit cycles was applied. The results were verified by an analogue simulation. Parametric and self-excited systems were classified by Yano

(1989) in three groups, depending on type of nonlinear terms. By applying the harmonic balance method regular motions near the main and fundamental parametric resonances for each class were compared. Rayleigh-Mathieu's one-degree-of-freedom oscillators with the influence of an external harmonic force or inertial excitation were investigated by Szabelski and Warmiński (1995a,b). The amplitudes of regular vibration and a new effect of additional solutions in the main parametric resonance were presented as well.

The review of the literature concludes that the transition from regular motion to chaos was intensively analysed in externally forced self-excited systems. Nevertheless, the results cannot be applied directly to parametric and self-excited systems. The main goal of this paper is to present new results for a simple one-degree of freedom oscillator, which includes three different types of excitation, i.e., self-excitation, parametric excitation and forced by an additional external harmonic force.

### 2. Model of the vibrating system

Let us consider a one-degree-of-freedom oscillator, which consists of a non-linear spring with periodically changing stiffness and nonlinear damping described by the van der Pol model. Let us assume that an external harmonic force can additionally force the oscillator (Fig. 1).

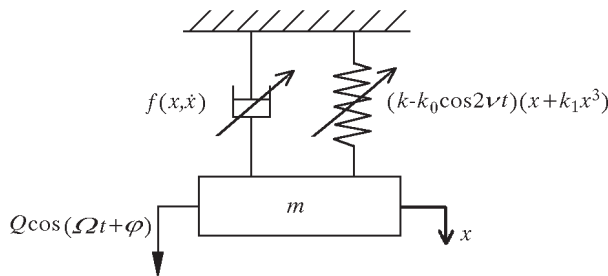


Fig. 1. Physical model of the van der Pol-Mathieu oscillator

The differential equation of motion of the oscillator has the form

$$mx'' + f(x, x') + (k - k_0 \cos 2\nu t)(x + k_1 x^3) = \begin{cases} 0 \\ Q \cos(\Omega t + \varphi) \end{cases} \quad (2.1)$$

where  $f(x, x')$  denotes the van der Pol function

$$f(x, x') = (-c_1 + \hat{c}_1 x^2)x'$$

Introducing the dimensionless time  $\tau = pt$  and a new dimensionless coordinate  $X = x/x_{st}$ , where  $p = \sqrt{k/m}$  is the natural frequency of the linear system and  $x_{st} = mg/k$  means the static displacement, we get

$$\ddot{X} + F_d(X, \dot{X}) + (1 - \mu \cos 2\vartheta\tau)(X + \gamma X^3) = \begin{cases} 0 \\ q \cos(\omega\tau + \varphi) \end{cases} \quad (2.2)$$

In equation (2.2) the following notation is applied

$$\begin{aligned} \alpha &= \frac{c_1}{mp} & \beta &= \frac{c_2 p}{m} x_{st}^2 & \gamma &= k_1 x_{st}^2 & \mu &= \frac{k_0}{k} \\ q &= \frac{Q}{m x_{st}} & \vartheta &= \frac{\nu}{p} & \omega &= \frac{\Omega}{p} \end{aligned}$$

The function  $F_d(X, \dot{X})$  is the dimensionless van der Pol damping function

$$F_d(X, \dot{X}) = (-\alpha + \beta X^2)\dot{X}$$

To find the analytical solutions we assumed that our system is weakly nonlinear and the parameters of the system are expressed by the formal small parameter  $\varepsilon$

$$\begin{aligned} F_d(X, \dot{X}) &= \varepsilon \tilde{F}_d(X, \dot{X}) & \alpha &= \varepsilon \tilde{\alpha} & \beta &= \varepsilon \tilde{\beta} \\ \gamma &= \varepsilon \tilde{\gamma} & \mu &= \varepsilon \tilde{\mu} & q &= \varepsilon \tilde{q} \end{aligned} \quad (2.3)$$

Then, we can write the differential equation of motion in the form

$$\begin{aligned} \ddot{X} + X &= \varepsilon \left\{ \tilde{F}_d(X, \dot{X}) + \tilde{\mu} \cos 2\vartheta\tau X - \tilde{\gamma} X^3 + \tilde{q} \cos(\omega\tau + \varphi) \right\} + \\ &+ \varepsilon^2 \tilde{\gamma} \tilde{\mu} X^3 \cos 2\vartheta\tau \end{aligned} \quad (2.4)$$

For  $\varepsilon$  equal to zero equation (2.4) describes vibrations of the linear oscillator with the natural frequency  $p$  equal to 1. For a nonlinear system ( $\varepsilon \neq 0$ ) we have to take into account the first and second order nonlinear terms.

### 3. Perturbation analysis

Analytical examinations of the considered parametric and self-excited system were carried out by applying multiple scale of time method (Nayfeh, 1981). All analytical calculations were made in Mathematica 3.0 package. At the beginning we define different time scales

$$T_n = \varepsilon^n \tau \quad n = 0, 1, 2, \dots$$

where  $T_0$  is a fast scale of time and  $T_1, T_2, \dots$  are slower scales of time. Then, the time derivatives are expressed by the formulae

$$\frac{d}{d\tau} = D_0 + \varepsilon D_1 + \dots \quad \frac{d^2}{d\tau^2} = D_0^2 + 2\varepsilon D_0 D_1 + \dots$$

where  $D_n^m = \partial^m / \partial T_n^m$  means the  $m$ th order partial derivative for  $n$ th order scale of time. In analytical calculations  $\varepsilon$  is still used as the small parameter.

Solution to (2.4) is expressed in the form

$$X(\tau, \varepsilon) = X_0(T_0, T_1, T_2) + \varepsilon X_1(T_0, T_1, T_2) + \varepsilon^2 X_2(T_0, T_1, T_2) + \dots \quad (3.1)$$

Let us consider the solutions near the parametric resonances. Then the parametric frequency  $\vartheta$  has to fulfil the condition

$$m\vartheta \approx np \quad (3.2)$$

where  $m$  and  $n$  are natural numbers and  $p$  is the natural frequency of the system.

In our case, after introducing the dimensionless time,  $p = 1$ , we can write around the parametric resonances

$$\frac{m^2}{n^2} \vartheta^2 = 1 + \varepsilon \sigma_1 \quad (3.3)$$

Taking into account (3.3) we have

$$\begin{aligned} \ddot{X} + \frac{m^2}{n^2} \vartheta^2 X = \varepsilon \left[ \tilde{F}_d(X, \dot{X}) + \tilde{\mu} \cos 2\vartheta\tau X - \tilde{\gamma} X^3 + \right. \\ \left. + \sigma_1 X + \tilde{q} \cos(\omega\tau + \varphi) \right] + \varepsilon^2 \tilde{\gamma} \tilde{\mu} X^3 \cos 2\vartheta\tau \end{aligned} \quad (3.4)$$

Putting solution (3.1) into (3.4) and grouping the terms with the same power of  $\varepsilon$  we obtain a system of consecutive perturbation equations:

— equation of the  $\varepsilon^0$  order

$$D_0^2 X_0 + \frac{m^2}{n^2} \vartheta^2 X_0 = 0 \quad (3.5)$$

— equation of the  $\varepsilon^1$  order

$$D_0^2 X_1 + \frac{m^2}{n^2} \vartheta^2 X_1 = \sigma_1 X_0 - 2D_0 D_1 X_0 + \tilde{F}_{d0} - \tilde{\gamma} X_0^3 + \\ + \tilde{\mu} X_0 \cos 2\vartheta\tau + \tilde{q} \cos(\omega\tau + \varphi) \quad (3.6)$$

— equation of the  $\varepsilon^2$  order

$$D_0^2 X_2 + \frac{m^2}{n^2} \vartheta^2 X_2 = \sigma_1 X_1 - D_1^2 X_0 - 2D_0 D_1 X_1 - 2D_0 D_2 X_0 + \\ + \tilde{F}_{d1} - 3\tilde{\gamma} X_0^2 X_1 + \tilde{\mu} X_1 \cos 2\vartheta\tau + \tilde{\gamma} \tilde{\mu} X_0^3 \cos 2\vartheta\tau \quad (3.7)$$

where

$$\tilde{F}_{d0} = \tilde{\alpha} D_0 X_0 - \tilde{\beta} D_0 X_0 X_0^2 \\ \tilde{F}_{d1} = \tilde{\alpha} (D_0 X_1 + D_1 X_0) - \tilde{\beta} (X_0^2 D_0 X_1 - X_0^2 D_1 X_0 + 2X_0 X_1 D_0 X_0)$$

Further analysis will be carried out for the main parametric resonance around the frequency  $\vartheta \approx 1$ . Influence of the external force will be considered in a particular case when the external force frequency  $\omega = \vartheta$  and the phase  $\varphi = 0$ . According to (3.3) for  $m = 1$ ,  $n = 1$  we can write

$$\vartheta^2 = 1 + \varepsilon\sigma_1 \quad (3.8)$$

Then solution to equation (3.5) is expressed in the exponential form

$$X_0(T_0, T_1, T_2) = A(T_1, T_2) \exp(i\vartheta T_0) + \bar{A}(T_1, T_2) \exp(-i\vartheta T_0) \quad (3.9)$$

where  $\bar{A}(T_1, T_2)$  is the complex conjugate function to  $A(T_1, T_2)$ .

Putting solution (3.9) into (3.6) we obtain

$$D_0^2 X_1 + \vartheta^2 X_1 = \left[ i\vartheta A(\tilde{\alpha} - \tilde{\beta} A \bar{A}) - 2i\vartheta D_1 A + \sigma_1 A - 3\tilde{\gamma} A^2 \bar{A} + \right. \\ \left. + \frac{1}{2} \tilde{\mu} \bar{A} + \tilde{q} \cos \vartheta\tau \right] \exp(i\vartheta T_0) + \left[ -(i\tilde{\beta}\vartheta + \tilde{\gamma}) A^3 + \frac{1}{2} \tilde{\mu} A \right] \exp(3i\vartheta T_0) + c.c. \quad (3.10)$$

where *c.c.* means complex conjugate terms.

The condition of secular terms elimination leads to the relation

$$i\vartheta A(\tilde{\alpha} - \tilde{\beta}A\bar{A}) - 2i\vartheta D_1 A + \sigma_1 A - 3\tilde{\gamma}A^2\bar{A} + \frac{1}{2}\tilde{\mu}\bar{A} + \frac{1}{2}\tilde{q} = 0 \tag{3.11}$$

The particular solution to equation (3.10) has the form

$$X_1 = \frac{1}{8\vartheta^2} A \left( i\tilde{\beta}\vartheta A^2 + \tilde{\gamma}A^2 - \frac{\tilde{\mu}}{2} \right) \exp(3i\vartheta T_0) \tag{3.12}$$

Introducing solution (3.12) into equation (3.7) we get

$$D_0^2 X_2 + \vartheta^2 X_2 = - \left[ \begin{aligned} & D_1^2 A + 2i\vartheta D_2 A + (-\tilde{\alpha} + 2\tilde{\beta}A\bar{A})D_1 A + \tilde{\beta}A^2 D_1 \bar{A} - \\ & - \frac{3}{2}\tilde{\gamma}\tilde{\mu}A\bar{A}^2 \left( \frac{1}{8\vartheta^2} + 1 \right) + \left( -\frac{1}{8}\tilde{\beta}^2 + \frac{1}{\vartheta}i\tilde{\beta}\tilde{\gamma} + \frac{3\tilde{\gamma}^2}{8\vartheta^2} \right) A^3 \bar{A}^2 - \\ & - \frac{1}{2}\tilde{\gamma}\tilde{\mu}A^3 \left( \frac{1}{8\vartheta^2} + 1 \right) + \frac{\tilde{\mu}^2}{32\vartheta^2} A \end{aligned} \right] \exp(i\vartheta T_0) - \tag{3.13}$$

$$- \left[ \begin{aligned} & \left( -\frac{3}{8}i\tilde{\mu} + \frac{9}{4\vartheta}i\tilde{\gamma}A^2 - \frac{5}{4}\tilde{\beta}A^2 \right) D_1 A + \\ & + \frac{1}{4}\tilde{\alpha}A^3 \left( \frac{3}{2}\tilde{\beta} - \frac{3}{\vartheta}i\tilde{\gamma} + \frac{3}{2\vartheta}i\tilde{\mu} \right) + \frac{1}{16\vartheta^2}\tilde{\mu}\sigma_1 A - \\ & - \frac{1}{8\vartheta}A^3 \left( 7i\tilde{\beta}\tilde{\mu} + \frac{1}{\vartheta}\tilde{\gamma}\sigma_1 \right) - \frac{3}{4}A^4 \bar{A} \left( \tilde{\beta}^2 + \frac{1}{\vartheta^2}\tilde{\gamma}^2 \right) + \\ & + \frac{3}{\vartheta}i\tilde{\beta}\tilde{\gamma}A^4 \bar{A} - \frac{3}{2}\tilde{\gamma}\tilde{\mu}A^2 \bar{A} \left( \frac{1}{4\vartheta^2} + 1 \right) \end{aligned} \right] \exp(3i\vartheta T_0) -$$

$$- \left[ \begin{aligned} & -\frac{5}{24}i\tilde{\alpha}\tilde{\mu}A + \frac{1}{32\vartheta^2}\tilde{\mu}^2 A - \frac{1}{2}\tilde{\gamma}\tilde{\mu}A^3 \left( \frac{1}{2\vartheta^2} + 1 \right) + \\ & + \left( \frac{3}{8\vartheta^2}\tilde{\gamma}^2 - \frac{5}{8}\tilde{\beta}^2 + \frac{2}{\vartheta}i\tilde{\beta}\tilde{\gamma} \right) A^5 - \frac{25}{24\vartheta}i\tilde{\beta}\tilde{\mu}A^2 \bar{A} \end{aligned} \right] \exp(5i\vartheta T_0) + c.c.$$

From elimination of secular terms in the solution to equation (3.13) we have

$$D_1^2 A + 2i\vartheta D_2 A + (-\tilde{\alpha} + 2\tilde{\beta}A\bar{A})D_1 A + \tilde{\beta}A^2 D_1 \bar{A} - \frac{3}{2}\tilde{\gamma}\tilde{\mu}A\bar{A}^2 \left( \frac{1}{8\vartheta^2} + 1 \right) + \tag{3.14}$$

$$+ \left( -\frac{1}{8}\tilde{\beta}^2 + \frac{1}{\vartheta}i\tilde{\beta}\tilde{\gamma} + \frac{3\tilde{\gamma}^2}{8\vartheta^2} \right) A^3 \bar{A}^2 - \frac{1}{2}\tilde{\gamma}\tilde{\mu}A^3 \left( \frac{1}{8\vartheta^2} + 1 \right) + \frac{\tilde{\mu}^2}{32\vartheta^2} A = 0$$

Applying the reconstitution method (Sanchez and Nayfeh, 1990) we transform equations (3.11) and (3.14) into one first order differential equation

$$\begin{aligned}
 & 2i\vartheta\dot{A} + \varepsilon\left(-i\tilde{\alpha}\vartheta A + i\tilde{\beta}\vartheta A^2\bar{A} - \sigma_1 A - \frac{1}{2}\tilde{\mu}\bar{A} + 3\tilde{\gamma}A^2\bar{A}\right) + \\
 & + \varepsilon^2 \left[ \begin{aligned} & \frac{1}{4}A\left(-\tilde{\alpha}^2 + \frac{3}{8\vartheta^2}\tilde{\mu}^2 - \frac{1}{\vartheta^2}\sigma_1^2\right) + \frac{3}{2\vartheta}A^2\bar{A}\left(i\tilde{\alpha}\tilde{\gamma} + \frac{1}{\vartheta}\tilde{\gamma}_1\sigma_1\right) - \\ & - A^3\bar{A}^2\left(\frac{7}{8}\tilde{\beta}^2 + \frac{1}{\vartheta}i\tilde{\beta}\tilde{\gamma} + \frac{15}{8\vartheta^2}\tilde{\gamma}^2\right) - \frac{1}{2}\tilde{\gamma}\tilde{\mu}A^3\left(\frac{7}{8\vartheta^2} + 1\right) + \\ & + \frac{1}{16}i\tilde{\beta}\tilde{\mu}A^3 + \frac{3}{2}\tilde{\gamma}\tilde{\mu}A\bar{A}^2\left(\frac{1}{8\vartheta^2} + 1\right) - \frac{3}{16\vartheta}i\tilde{\beta}\tilde{\mu}A\bar{A}^2 \end{aligned} \right] + \\
 & + \varepsilon^2\tilde{q} \left[ \begin{aligned} & -\frac{1}{8\vartheta^2}\sigma_1 + \frac{1}{8\vartheta}\tilde{\alpha} + \frac{1}{16\vartheta^2}\tilde{\mu} + \frac{3}{4\vartheta^2}\tilde{\gamma}\left(A\bar{A} - \frac{1}{2}A^2\right) + \\ & + \frac{1}{4\vartheta}\tilde{\beta}\left(\frac{1}{2}A^2 - A\bar{A}\right) \end{aligned} \right] = 0
 \end{aligned} \tag{3.15}$$

The variable  $A$  is expressed as the exponential function

$$A = \frac{1}{2}a \exp(i\Phi) + \frac{1}{2}a \exp(-i\Phi) \tag{3.16}$$

where  $a$  and  $\Phi$  are vibration amplitude and phase, respectively.

Substituting (3.16) into (3.15) and then separating the real and imaginary parts we get two first order modulation equations

$$\begin{aligned}
 \dot{a} = & \frac{1}{2}\varepsilon\tilde{\alpha}a - \frac{3}{16\vartheta^2}\varepsilon^2\tilde{\alpha}\tilde{\gamma}a^3 - \frac{1}{8}\varepsilon\tilde{\beta}a^3 + \frac{1}{32\vartheta^2}\varepsilon^2\tilde{\beta}\tilde{\gamma}a^5 + \frac{1}{64\vartheta^2}\varepsilon^2\tilde{\beta}\tilde{\mu}a^3 \cos 2\Phi + \\
 & + \frac{1}{4\vartheta}\varepsilon\tilde{\mu}a\left(-1 + \frac{5}{16\vartheta^3}\varepsilon\tilde{\gamma}a^2 - \frac{1}{2}\varepsilon\tilde{\gamma}a^2\right) \sin 2\Phi + \\
 & + \varepsilon\tilde{q}\frac{1}{8\vartheta}\left[\frac{1}{\vartheta}\varepsilon\left(-\tilde{\alpha} + \frac{1}{4}\tilde{\beta}a^2\right) \cos \Phi - \left(5 - \frac{1}{\vartheta^2} - \frac{9}{4\vartheta^2}\varepsilon\tilde{\gamma}a^2 + \frac{1}{\vartheta^2}\varepsilon\tilde{\mu}\right) \sin \Phi\right]
 \end{aligned} \tag{3.17}$$

$$\begin{aligned}
 a\dot{\Phi} = & \frac{1}{8\vartheta}\varepsilon^2\tilde{\alpha}a\left(-\tilde{\alpha} + \tilde{\beta}a^2\right) - \frac{a}{8\vartheta}\left[(-1 + \vartheta^2)\left(5 - \frac{1}{\vartheta^2}\right) - \frac{3}{8\vartheta^2}\varepsilon^2\tilde{\mu}^2\right] + \\
 & + a^3\left(\frac{3}{8\vartheta}\varepsilon\tilde{\gamma} + \frac{3}{16\vartheta^3}\varepsilon\tilde{\gamma}\left(-1 + \vartheta^2\right)\right) - \frac{1}{256\vartheta}\varepsilon^2a^5\left(7\tilde{\beta}^2 + \frac{15}{\vartheta^2}\tilde{\gamma}^2\right) - \\
 & - \frac{1}{32\vartheta^2}\varepsilon\tilde{\beta} \sin 2\Phi - \frac{1}{4\vartheta}\varepsilon\tilde{\mu}a\left[1 + \left(\frac{1}{8\vartheta^2} + 1\right)\varepsilon\tilde{\gamma}a^2\right] \cos 2\Phi + \\
 & + \varepsilon\tilde{q}\frac{1}{8\vartheta}\left[\left(-5 + \frac{1}{\vartheta^2} + \frac{3}{8\vartheta^3}\varepsilon\tilde{\gamma}a^2 + \frac{1}{\vartheta^2}\varepsilon\tilde{\mu}\right) \cos \Phi + \frac{1}{\vartheta}\varepsilon\left(-\tilde{\alpha}^2 + \tilde{\beta}a^2\right) \sin \Phi\right]
 \end{aligned}$$

Basing on equation (3.1) an approximate solution has the form

$$\begin{aligned}
 X = a \cos(\vartheta\tau + \Phi) + \varepsilon \left[ \frac{1}{32\vartheta^2} \tilde{\gamma} a^3 \cos(3\vartheta\tau + 3\Phi) - \right. \\
 \left. - \frac{1}{16\vartheta^2} \tilde{\mu} a \cos(3\vartheta\tau + \Phi) - \frac{1}{32\vartheta} \tilde{\beta} a^3 \sin(3\vartheta\tau + 3\Phi) \right] \tag{3.18}
 \end{aligned}$$

For the steady state  $\dot{a} = 0, \dot{\Phi} = 0$ , and then from (3.17), we obtain bifurcation equations

$$\begin{aligned}
 \frac{1}{2} \varepsilon \tilde{\alpha} a - \frac{3}{16\vartheta^2} \varepsilon^2 \tilde{\alpha} \tilde{\gamma} a^3 - \frac{1}{8} \varepsilon \tilde{\beta} a^3 + \frac{1}{32\vartheta^2} \varepsilon^2 \tilde{\beta} \tilde{\gamma} a^5 + \frac{1}{64\vartheta^2} \varepsilon^2 \tilde{\beta} \tilde{\mu} a^3 \cos 2\Phi + \\
 + \frac{1}{4\vartheta} \varepsilon \tilde{\mu} a \left( -1 + \frac{5}{16\vartheta^3} \varepsilon \tilde{\gamma} a^2 - \frac{1}{2} \varepsilon \tilde{\gamma} a^2 \right) \sin 2\Phi = \\
 = \varepsilon \tilde{q} \frac{1}{8\vartheta} \left[ -\frac{1}{\vartheta} \varepsilon \left( -\tilde{\alpha} + \frac{1}{4} \tilde{\beta} a^2 \right) \cos \Phi + \left( 5 - \frac{1}{\vartheta^2} - \frac{9}{4\vartheta^2} \varepsilon \tilde{\gamma} a^2 + \frac{1}{\vartheta^2} \varepsilon \tilde{\mu} \right) \sin \Phi \right] \tag{3.19}
 \end{aligned}$$

$$\begin{aligned}
 \frac{1}{8\vartheta} \varepsilon^2 \tilde{\alpha} a \left( -\tilde{\alpha} + \tilde{\beta} a^2 \right) - \frac{a}{8\vartheta} \left[ \left( -1 + \vartheta^2 \right) \left( 5 - \frac{1}{\vartheta^2} \right) - \frac{3}{8\vartheta^2} \varepsilon^2 \tilde{\mu}^2 \right] + \\
 + a^3 \left[ \frac{3}{8\vartheta} \varepsilon \tilde{\gamma} + \frac{3}{16\vartheta^3} \varepsilon \tilde{\gamma} \left( -1 + \vartheta^2 \right) \right] - \frac{1}{256\vartheta} \varepsilon^2 a^5 \left( 7\tilde{\beta}^2 + \frac{15}{\vartheta^2} \tilde{\gamma}^2 \right) - \\
 - \frac{1}{32\vartheta^2} \varepsilon \tilde{\beta} \sin 2\Phi - \frac{1}{4\vartheta} \varepsilon \tilde{\mu} a \left[ 1 + \left( \frac{1}{8\vartheta^2} + 1 \right) \varepsilon \tilde{\gamma} a^2 \right] \cos 2\Phi = \\
 = \varepsilon \tilde{q} \frac{1}{8\vartheta} \left[ \left( 5 - \frac{1}{\vartheta^2} - \frac{3}{8\vartheta^3} \varepsilon \tilde{\gamma} a^2 - \frac{1}{\vartheta^2} \varepsilon \tilde{\mu} \right) \cos \Phi - \frac{1}{\vartheta} \varepsilon \left( -\tilde{\alpha}^2 + \tilde{\beta} a^2 \right) \sin \Phi \right]
 \end{aligned}$$

Equations (3.19) enable us to determine the amplitude  $a$  and phase  $\Phi$  for the steady state in the second order approximation. For parametrically and self-excited systems without external forces it is necessary to introduce  $q = 0$  and then the right-hand sides of the bifurcation equations become zero. Then the bifurcation points of the trivial into nontrivial solution for a system without the external force can be determined by putting  $a = 0$  and rearranging equations (3.19)

$$\begin{aligned}
 \frac{1}{4} - 3\vartheta^2 + \frac{23}{2} \vartheta^4 - 15\vartheta^6 + \frac{25}{4} \vartheta^8 + \\
 + \varepsilon^2 \left( \frac{1}{2} \tilde{\alpha}^2 \vartheta^2 - 3\tilde{\alpha}^2 \vartheta^4 + \frac{13}{2} \tilde{\alpha}^2 \vartheta^6 - \frac{3}{16} \tilde{\mu}^2 + \frac{9}{8} \vartheta^2 \tilde{\mu}^2 - \frac{31}{16} \vartheta^4 \tilde{\mu}^2 \right) + \tag{3.20} \\
 + \varepsilon^4 \left( \frac{1}{4} \tilde{\alpha}^4 \vartheta^4 - \frac{3}{16} \tilde{\alpha}^2 \vartheta^2 \tilde{\mu}^2 + \frac{9}{256} \tilde{\mu}^4 \right) = 0
 \end{aligned}$$

One can notice that the bifurcation points found from (3.20) do not depend on the parameter  $\beta$ . Considering only the first order perturbation equation (3.11) we find a resonance curve in the direct form

$$(1 - \vartheta^2)^2 + \varepsilon^2 \left( \tilde{\alpha}^2 \vartheta^2 - \frac{\tilde{\mu}^2}{4} \right) + \left[ -\frac{1}{2} \varepsilon^2 \tilde{\alpha} \tilde{\beta} \vartheta^2 + \frac{3}{2} \varepsilon \tilde{\gamma} (1 - \vartheta^2) \right] a^2 + \varepsilon^2 \left( \frac{9}{16} \tilde{\gamma}^2 + \frac{1}{16} \tilde{\beta}^2 \vartheta^2 \right) a^4 = 0 \tag{3.21}$$

and hence we get the amplitude and the phase of stable vibrations

$$a = \sqrt{\frac{-\left(-\frac{1}{2} \varepsilon^2 \tilde{\alpha} \tilde{\beta} \vartheta^2 + \frac{3}{2} \varepsilon \tilde{\gamma} (1 - \vartheta^2)\right) \mp \sqrt{d_1}}{2 \varepsilon^2 \left(\frac{9}{16} \tilde{\gamma}^2 + \frac{1}{16} \tilde{\beta}^2 \vartheta^2\right)}} \tag{3.22}$$

$$\tan \Phi = \frac{\varepsilon \vartheta (4 \tilde{\alpha} - \tilde{\beta} a^2)}{4 - 4 \vartheta^2 + 3 \tilde{\gamma} \varepsilon a^2}$$

where

$$d_1 = \left[ -\frac{1}{2} \varepsilon^2 \tilde{\alpha} \tilde{\beta} \vartheta^2 + \frac{3}{2} \varepsilon \tilde{\gamma} (1 - \vartheta^2) \right]^2 - 4 \varepsilon^2 \left( \frac{9}{16} \tilde{\gamma}^2 + \frac{1}{16} \tilde{\beta}^2 \vartheta^2 \right) \left[ (1 - \vartheta^2)^2 + \varepsilon^2 \left( \tilde{\alpha}^2 \vartheta^2 - \frac{\tilde{\mu}^2}{4} \right) \right]$$

For  $a = 0$  from (3.21) we have

$$1 - 2 \vartheta^2 + \vartheta^4 + \varepsilon^2 \left( \tilde{\alpha}^2 \vartheta^2 - \frac{\mu^2}{4} \right) = 0 \tag{3.23}$$

and then the bifurcation points of the trivial into non-trivial solution in the first order approximation are

$$\vartheta_{1,2}^* = \sqrt{\frac{2 - \varepsilon^2 \tilde{\alpha}^2 \mp \varepsilon \sqrt{-4 \tilde{\alpha}^2 + \varepsilon^2 \tilde{\alpha}^4 + \tilde{\mu}^2}}{2}} \tag{3.24}$$

The points described by (3.24) can appear if  $-4 \tilde{\alpha}^2 + \varepsilon^2 \tilde{\alpha}^4 + \tilde{\mu}^2 > 0$ . It means that the shape of the resonance curve depends on the self-excitation  $\alpha$  and the parametric excitation  $\mu$ . Assuming that  $\varepsilon$  is a small parameter we can neglect the term  $\varepsilon^2 \tilde{\alpha}^4$  as a small value, and then determine the condition

$$\frac{\mu}{\alpha} \geq 2 \tag{3.25}$$

which must be satisfied in order to get the bifurcation points. This is in agreement with the result obtained by Szabelski and Warmiński (1995a,b) for Rayleigh's model. In the opposite case, if condition (3.25) is not satisfied, the resonance curve has a closed form and lies above the  $\vartheta$  axis. Analysing (3.22)<sub>1</sub> we can define the conditions when the parametric resonance does not take place. Such situations can appear if it is not possible to have a real solution for the vibration amplitude, i.e. when  $d_1$  is smaller than zero.

#### 4. Regular vibration, numerical examples

Exemplary calculations were made by using analytical dependencies and numerical simulation. Numerical data were based on the papers by Tondl (1978), Yano (1989), Szabelski and Warmiński (1995a) which concerned self- and parametrically excited systems. The basic data are following

$$\alpha = 0.01 \qquad \beta = 0.05 \qquad \gamma = 0.1 \qquad \mu = 0.2$$

First, we examine vibration of the system without the external force ( $q = 0$ ) and near the main parametric resonance region. Fig. 2 presents a resonant curve obtained from the perturbation analysis (index AR) and numerical simulation (RKG). Near the main parametric resonance we observe the synchronisation phenomenon. In this region the parametric vibrations pull in the self-excited ones and the system vibrates only with the single frequency  $\vartheta$  equal to the half of the parametric excitation frequency  $2\vartheta$ . The analytical solution is plotted by the solid or dashed line for stable and unstable solutions, respectively. Outside the synchronisation area the system vibrates quasi-periodically. Then the response of the system includes strong influence of self-excitation and we observe vibration with modulated amplitude. This kind of vibration consists of two signals, whose frequency ratio is not a rational number. On the phase plane such motion is represented by stable quasi-periodic limit cycles.

Double points outside the resonance region denote extreme values of the modulated amplitude. The amplitude and phase modulation is determined by equations (3.17). We can observe behaviour of the system for increasing parametric frequency  $\vartheta$  from  $\vartheta = 0.8$  up to  $\vartheta = 1.5$ . At the beginning ( $\vartheta \approx 0.8$ ) the system vibrates quasi-periodically, then, around  $\vartheta^* = 0.9489$ , the first nontrivial steady but unstable solution appears (the first bifurcation point of the trivial into nontrivial solution). This unstable region (unstable focus) is

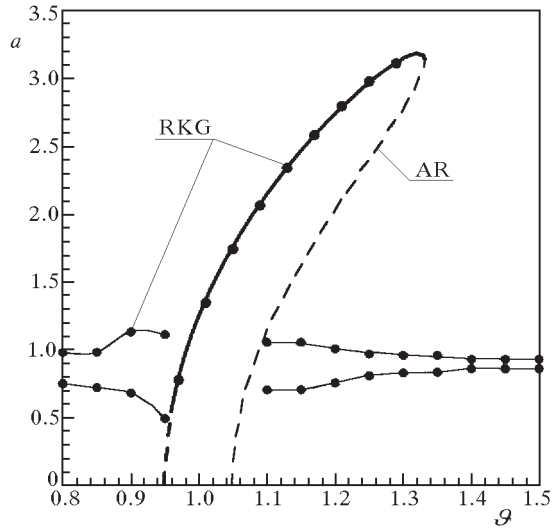


Fig. 2. Synchronisation area around the main parametric resonance, AR – analytical results, RKG – numerical simulation

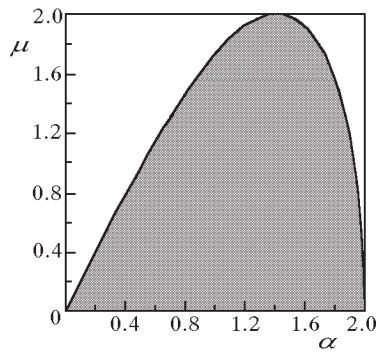


Fig. 3. Bifurcation values of  $\mu$  and  $\alpha$  parameters

very small, between  $\vartheta = 0.95$  and  $\vartheta = 0.96$  (dashed line in Fig. 2). Next, the solution transits to a stable focus. The synchronisation region starts in the point where the steady state is stable and the system vibrates periodically with the single  $\vartheta$  frequency. Above the frequency  $\vartheta = 1.0486$  (the second bifurcation point) an unstable saddle point appears in the synchronisation region. Next, after passing  $\vartheta = 1.1$  an additional quasi-periodic solution represented by a stable quasi-periodic limit cycle occurs. In the region  $\vartheta \in (1.1, 1.3)$  we obtain periodic and quasi-periodic solutions, depending on initial conditions. The saddle points divide the phase space into two basins of an attractor. Above  $\vartheta = 1.3$  the system leaves the synchronisation region and vibrates quasi-periodically.

From practical point of view, it is important to determine the parameters influencing the synchronisation width and vibration amplitudes. Analytical dependencies enable us to find the critical value of  $\mu$  and  $\alpha$  parameters where the bifurcation points disappear. The grey area in Fig. 3 corresponds to condition (3.24) and for such parameters that the resonance curve has a closed form and no points belonging to the  $\vartheta$  axis. For small values of the parameters  $\alpha, \mu$  the limit region in Fig. 3 is determined by the slope of a straight line  $\mu/\alpha = 2$ .

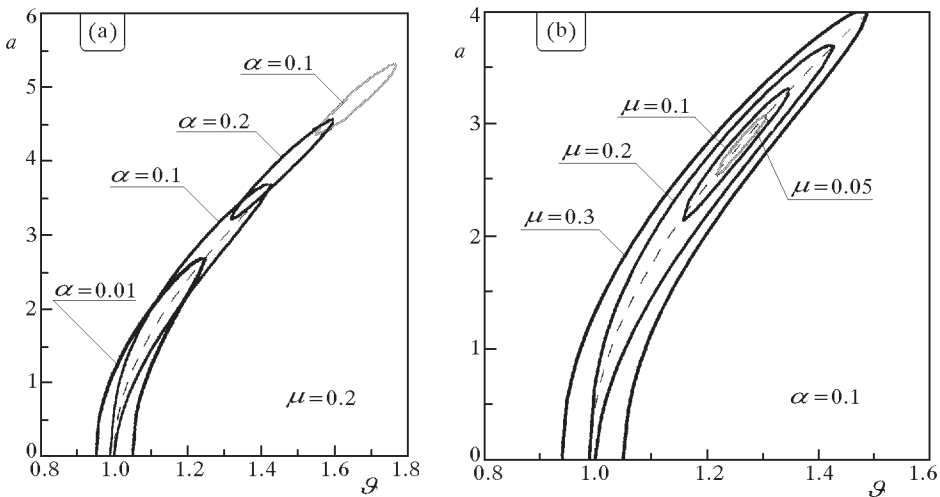


Fig. 4. Influence of  $\alpha$  and  $\mu$  parameters on the resonance curve around the main parametric resonance

The influence of the  $\alpha$  parameter on the resonance curve is presented in Fig. 4a. For  $\alpha = 0.01, \mu = 0.2$  the resonance curve has two bifurcation points,

for  $\alpha = 0.1$  the bifurcation points are very close one to another ( $\alpha/\mu = 2$ ), for  $\alpha = 0.2$ ,  $\alpha = 0.3$  the resonance curve has a closed form and lies above the  $\vartheta$  axis (grey region in Fig. 3). An increase in the parameter  $\alpha$ , which is connected with self-excitation, causes an increase in the vibration amplitude and reduction in the width of the synchronisation region. For greater values of  $\alpha$  the synchronisation area moves along a skeleton line towards higher values of the excitation frequency  $\vartheta$ . The influence of the parametric excitation is different. In Fig. 4b we can observe resonance curves for the constant value  $\alpha = 0.1$  and variable  $\mu$  parameter. Generally, decreasing of the parametric excitation causes decreasing of the vibration amplitude and decreasing of the width of the synchronisation region. Nevertheless, the centre of the resonance remains permanently in the same place.

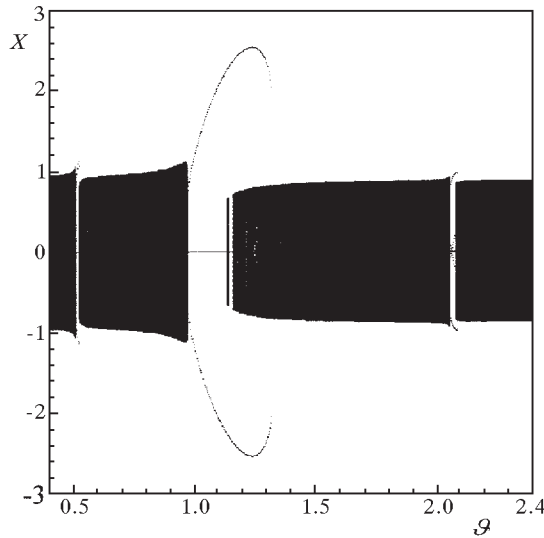


Fig. 5. Bifurcation diagram versus  $\vartheta$  parameter

The bifurcation diagram versus the  $\vartheta$  parameter (Fig. 5) obtained from a numerical simulation confirms the analytical results. The black regions correspond to quasi-periodic motion, while the single lines correspond to synchronisation regions. We can notice three resonance areas in the considered  $\vartheta$  interval, i.e. the main parametric resonance around  $\vartheta \approx 1.0$ , and the two second order resonances around  $\vartheta \approx 1/2$  and  $\vartheta \approx 2$ . The most dominating synchronisation region is near the main parametric resonance. The two additional regions are almost invisible. The synchronisation width and amplitude are much smaller than for the main parametric resonance. Therefore, in

Section 6, we decided to examine the influence of the external force on the vibrating system exactly in the main parametric resonance region.

### 5. Chaotic vibrations

Analysis of chaotic vibrations was based on numerical simulations by using the Dynamics package (Nusse and York, 1994). Numerical calculations of the parametric and self-excited system were made for the parameters  $\alpha = 0.01$ ,  $\beta = 0.05$ ,  $\gamma = 0.1$ ,  $\vartheta = 1.0$ , but for larger values of the parametric excitation amplitude  $\mu$ . First, a bifurcation diagram and maximal Lyapunov's exponent in the region  $\mu \in < 0, 2 >$  for the system without an external excitation  $q = 0$ , was calculated (Fig. 6).

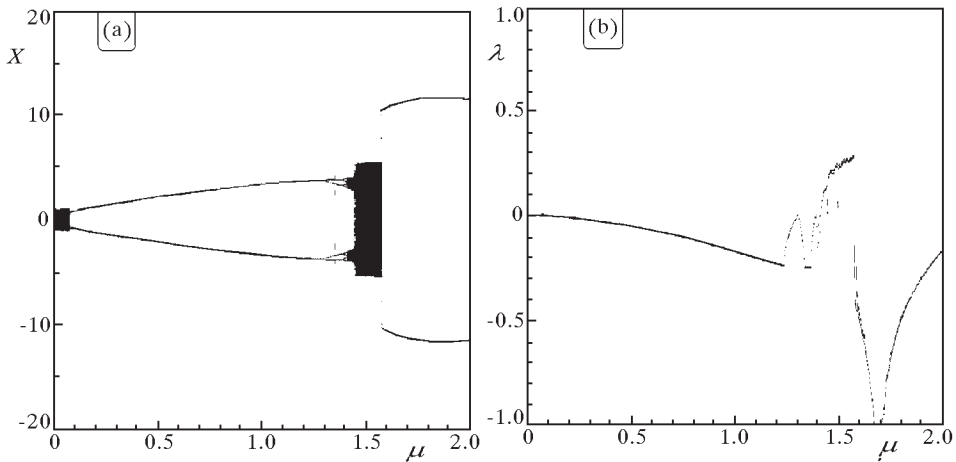


Fig. 6. Bifurcation diagram (a) and maximal Lyapunov's exponent (b) versus  $\mu$  parameter

For small values of the parametric excitation the oscillator vibrates quasi-periodically (black regions in Fig. 6a). Maximal Lyapunov's exponent for this type of motion is equal to zero (Fig. 6b). For  $\mu \approx 0.08$  the system transits from quasi-periodic to periodic motion represented by two lines on the bifurcation diagram. There, the Hopf bifurcation takes place. In a wide region  $\mu \in (0.08, 1.3)$  the system vibrates purely periodically. There are no qualitative changes in the bifurcation diagram in this region. Near  $\mu = 1.3$  we observe the first "pitchfork" bifurcation. A further increase in the  $\mu$  parame-

ter, causes next pitchfork bifurcations, and around  $\mu = 1.40$  after a cascade of bifurcations, the system passes from regular to chaotic motion. In the region  $\mu \in (1.41, 1.57)$  maximal Lyapunov's exponent is positive (Fig. 6b). It means that the system vibrates chaotically. Near  $\mu = 1.57$  after the "crisis" bifurcation the system directly jumps from chaotic motion to periodic one.

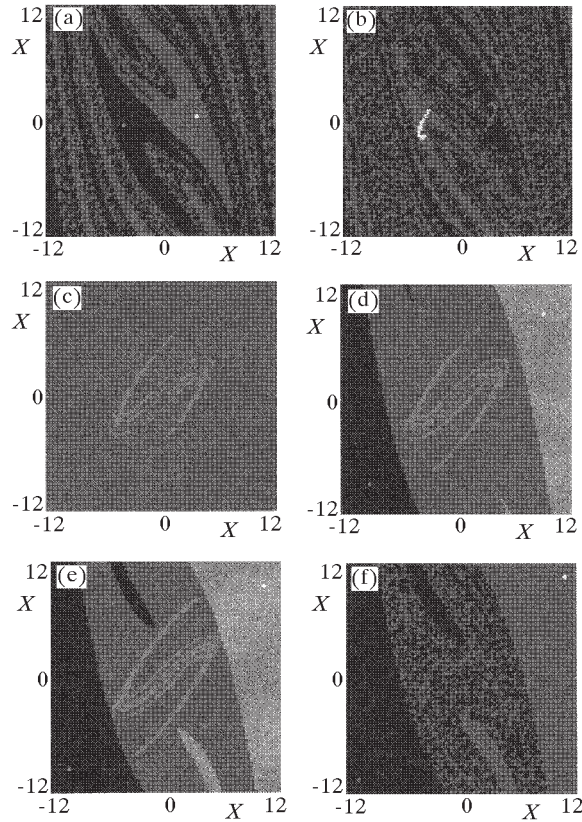


Fig. 7. Basins of attraction evolution near chaotic region; (a)  $\mu = 1.30$ , (b)  $\mu = 1.43$ , (c)  $\mu = 1.45$ , (d)  $\mu = 1.49$ , (e)  $\mu = 1.55$ , (f)  $\mu = 1.60$

Topological changes of the attractor during the transition through chaotic motion are presented in Fig. 7. We can observe the attractors as well as evolution of their basins. In the region of regular motion for  $\mu = 1.3$  (Fig. 7a) we obtain regular attractors as two points with two different basins. When we come into the chaotic area those regular points change into two small separate strange chaotic attractors and their basins become strongly mixed (Fig. 7b). Next, the two attractors join themselves into one large strange chaotic attrac-

tor. There is only one basin in this area (Fig. 7c). After exceeding  $\mu = 1.486$ , apart from the chaotic attractors there appear two regular ones. The phase space is divided into three areas, two for regular motion and the third in the centre for chaotic one (Fig. 7d). Regular and chaotic motion coexists with each other. Two "tongues" in the central area appear. We observe a similar situation in Fig. 7e, however the influence of regular motion increases. After exceeding the parameter value  $\mu = 1.58$  the chaotic region is completely destroyed by the two "tongues" and we observe only the regular motion (Fig. 7f). The central region is mixed by two regular basins of the attractors.

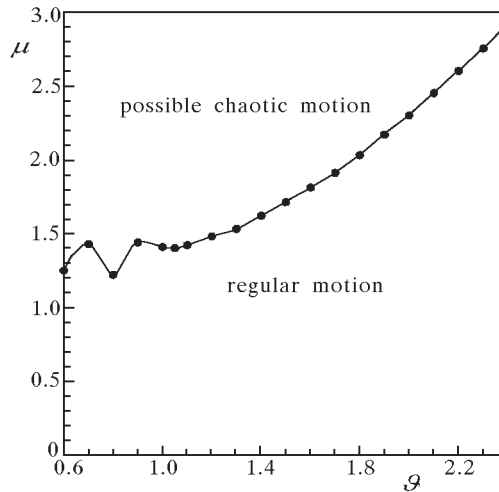


Fig. 8. Regions of appearance of regular and chaotic motion

The limit value of the amplitude and frequency of the parametric excitation where chaotic motion does not take place is presented in Fig. 8. Below the limit line the chaotic motion does not appear. The plane above that line is divided into smaller chaotic and regular regions. It was difficult to find precisely all chaotic subregions and, therefore, a criterion for regular motion was applied. Basing on the numerical investigations we can conclude that the chaotic motion can appear only if the value of the parametric excitation is greater than 1,  $\mu > 1$ .

## 6. Influence of external force on regular and chaotic motion

In Section 4 we showed that the synchronisation area near the main pa-

rametric region has the most important meaning. In this section we will investigate behaviour of the system when it is additionally forced by an external harmonic force. Let us assume that the amplitude of the external force  $q$  is not large and that the frequency  $\omega$  is equal to  $\vartheta$ , i.e. the external frequency is half of the parametric frequency value (2.4).

An approximate solution of the system with external excitation has form (3.1), however the amplitude and phase are described by (3.17). In the first order perturbation analysis the modulation equations take the form

$$\begin{aligned} \dot{a} &= \frac{1}{2}\varepsilon\tilde{\alpha}a - \frac{1}{8}\varepsilon\tilde{\beta}a^3 - \frac{1}{4\vartheta}\varepsilon\tilde{\mu}a \sin 2\Phi - \frac{1}{2\vartheta}\varepsilon\tilde{q} \sin \Phi \\ \dot{\Phi} &= -\frac{1}{2\vartheta}(-1 + \vartheta^2) + \frac{3}{8\vartheta}\varepsilon\tilde{\gamma}a^2 - \frac{1}{4\vartheta}\varepsilon\tilde{\mu} \cos 2\Phi - \frac{1}{2\vartheta a}\varepsilon\tilde{q} \cos \Phi \end{aligned} \tag{6.1}$$

We will present the influence of the external harmonic force on the system for the following numerical data

$$\alpha = 0.1 \qquad \beta = 0.05 \qquad \gamma = 0.1 \qquad \mu = 0.2 \qquad q = 0.2$$

The resonance curves obtained from (3.19) near the main parametric resonance are presented in Fig. 9.

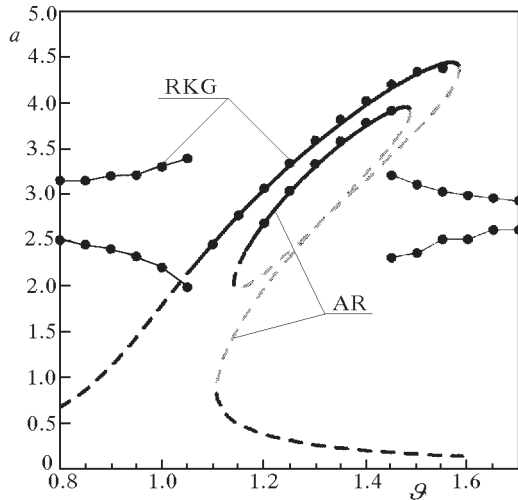


Fig. 9. Synchronisation area around the main parametric resonance; system with external excitation  $q = 0.2$

When a small external force additionally excites the system, we can observe significant differences in the synchronisation region. The amplitude-frequency

characteristic has not a typical shape. There is an additional internal loop in the considered region. Stability analysis shows that only the upper part of the internal loop is stable. There are five possible steady solutions inside the synchronisation regions. Nevertheless, only the two upper solutions are stable. This effect was also observed by Szabelski and Warmiński (1995a,b), in Rayleigh's model. Outside the synchronisation regions the system vibrates quasi-periodically. The two points, according to the extreme deflection of the system (Fig. 9) mark this type of motion. These stable additional solutions are visible also in the bifurcation diagrams versus the frequency  $\vartheta$  (Fig. 10).

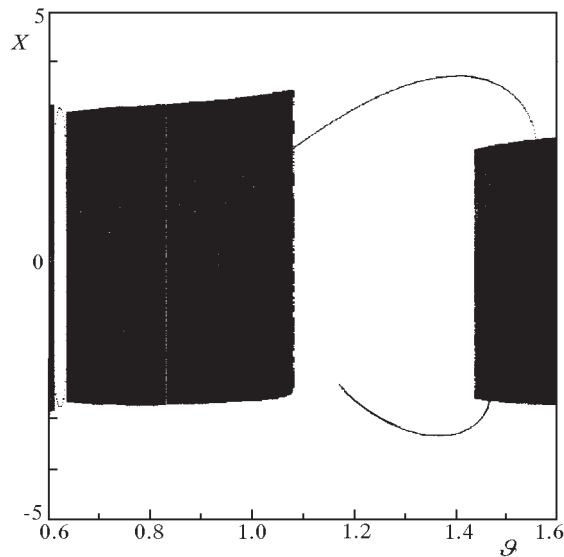


Fig. 10. Bifurcation diagram versus frequency  $\vartheta$ , system with external excitation  $q = 0.2$

The single line in Fig. 10 corresponds to synchronised vibrations and the black regions to quasi-periodic motion. The additional stable solution is located in the lower part of the plot. It means, that this solution has a different phase with respect to the upper solution. We can also notice that the external force causes an increase in the vibration amplitude in the synchronisation area and an increase in the vibration modulation outside this region. Fig. 11 presents the resonance curves versus the amplitude of the external force. One can notice that the internal loop in the synchronisation region near the main parametric resonance appears only as a result of action of a small external force.

The limit value for the van der Pol model is  $q = 0.7$ . For larger values

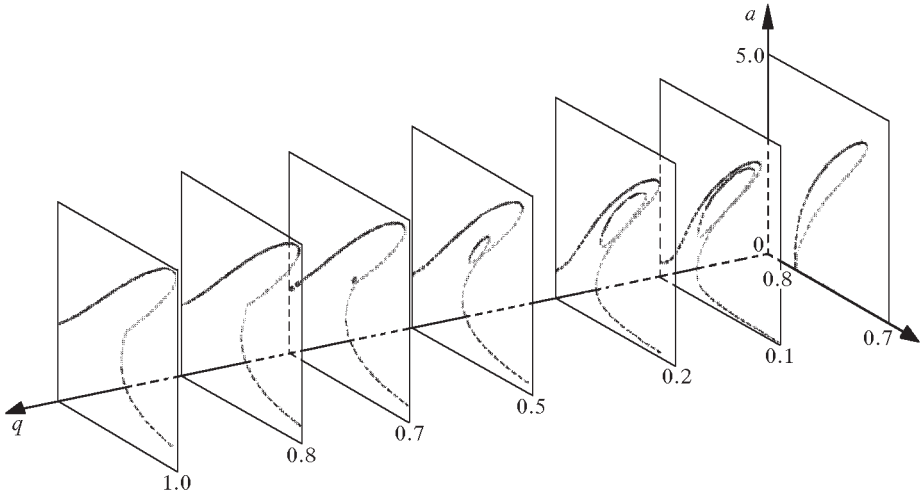


Fig. 11. Influence of the external force on the synchronisation area near the main parametric resonance

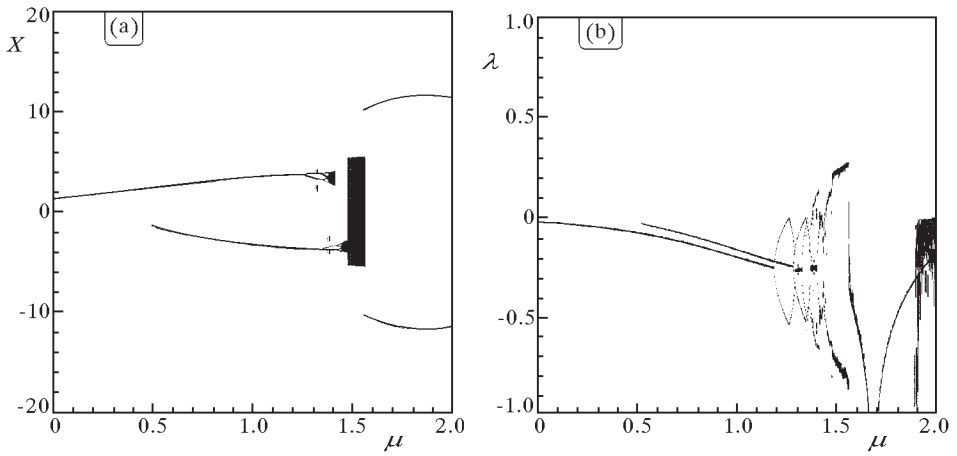


Fig. 12. System with external excitation; (a) bifurcation diagram, (b) Lyapunov's exponent versus  $\mu$  parameter

of the external force the internal loop completely disappears. Increasing of the amplitude of the external force makes the vibrations stable in a wider interval of  $\vartheta$  (synchronisation region is wider) and vibration amplitude slightly increasing.

The transition of the system to chaos with an additional external force is visible in the bifurcation diagrams in Fig. 12. In Fig. 12a the generalised coordinate  $X$  versus the  $\mu$  parameter was plotted for  $q = 0.2$ ,  $\vartheta = 1.0$ . Fig. 12b presents the diagram of the corresponding Lyapunov exponent. In comparison with Fig. 6 we can observe a symmetry breaking in the system. Bifurcations appear in two different regions of the  $\mu$  parameter, shifted relatively one to another. The system can vibrate along the upper or lower curve, depending on initial conditions. The region of quasi-periodic motion, which occurred for a small value of the  $\mu$  parameter for the system without an external force (Fig. 6), disappeared in Fig. 12. Lyapunov's exponent is negative in that region. Positive values of the Lyapunov exponent emerge around  $\mu = 1.45$ , similar to the system without an external force. Nevertheless, an additional external force decreases the chaotic area and divides it into two parts. This is an effect of asymmetry of the system as a result of the external force action. The influence of the external force on the chaotic motion can be investigated by observing the behaviour of one chosen strange chaotic attractor (for  $\mu = 1.45$ , Fig. 13) when the system is additionally excited by an external harmonic force. The amplitude of that force was changed in the interval  $q \in \langle 0, 1 \rangle$ . In Fig. 13 the coordinate  $X$  and Lyapunov exponent versus  $q$  is presented.

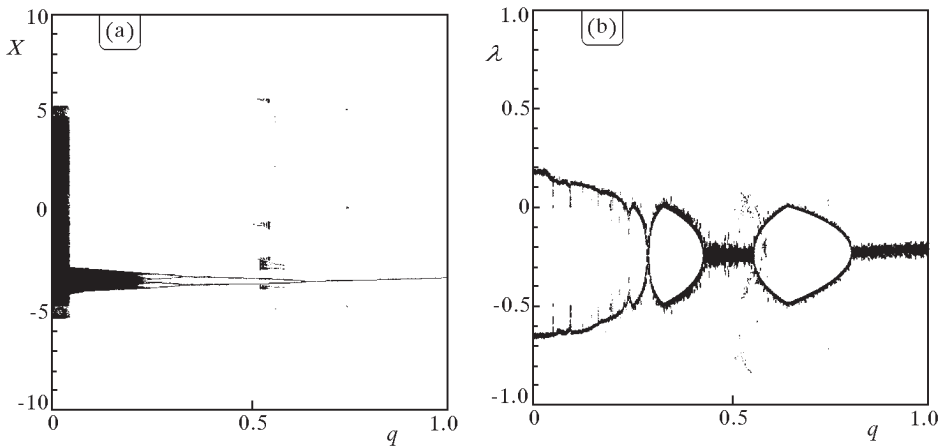


Fig. 13. Influence of the external force on chaotic vibration; (a) bifurcation diagram, (b) Lyapunov exponent versus  $q$  parameter

We can see that the external force removed chaos from the system. The strange attractor transits from chaos to regular motion via quasi-periodic motion. Maximal Lyapunov's exponent gradually tends from positive to negative values (Fig. 13b).

## 7. Summary and conclusion

The interaction between parametric and self-excited vibrations leads to synchronisation phenomena around the parametric resonances. In this paper vibrations near the main parametric resonance around  $\vartheta \approx 1$  are considered. Then, self-excited vibrations are pulled in by the parametric ones and the response of the system becomes purely harmonic. Outside that region the system vibrates quasi-periodically with a modulated amplitude. The synchronisation effect is most visible around the main parametric resonance. That region is the widest and the vibration amplitudes are the largest. It is also presented that the second order resonances are less important from practical point of view. Increasing of the parametric excitation  $\mu$  over 1 ( $\mu > 1$ ) can introduce van der Pol-Mathieu's oscillator to chaotic motion. Coexistence of chaotic and regular motions for the same parameter, depending on initial conditions, is also possible. The additional external force causes qualitative and quantitative changes in the synchronisation area around the main parametric resonance. For a small amplitude of the external force, there appears an additional internal loop in that region. Only the upper part of the loop is stable, the lower one is unstable. This result is similar to Rayleigh-Mathieu's oscillator obtained by Szabelski and Warmiński (1995a). The external force removes chaos from the considered system. Then we observe soft transition from chaotic to periodic motion through quasi-periodic one.

## References

1. AWREJCEWICZ J., 1990, Bifurkacje i chaos w układach dynamicznych, *Zeszyty Naukowe 383, Rozprawy Naukowe*, **127**, Politechnika Łódzka
2. AWREJCEWICZ J., 1996, *Drgania deterministyczne układów dyskretnych*, Wydawnictwa Naukowo-Techniczne, Warszawa

3. GUCKENHEIMER J., HOLMES P., 1997, Nonlinear Oscillations, Dynamical Systems, and Bifurcations of Vector Fields, *Applied Mathematical Sciences*, **42**, Springer-Verlag
4. HAYASHI CH., 1964, *Nonlinear Oscillations in Physical Systems*, McGraw-Hill, Inc
5. KAPITANIAK T., STEEB W.H., 1991, Transition to Hyperchaos in Coupled Generalized Van der Pol's Equations, *Physics Letters A*, **152**, 33-37
6. LITAK G., SPUZ-SZPOS G., SZABELSKI K., WARMIŃSKI J., 1999, Vibration of Externally Forced Froude Pendulum, *International Journal of Bifurcation and Chaos*, **9**, 3, 561-570
7. NAYFEH, A.,H., 1981, *Introduction to Perturbation Techniques*, John Wiley and Sons, New York
8. NUSSE H., YORK A., 1994, *Dynamics, Numerical Explorations*, Springer Verlag, New York
9. SANCHEZ N.E., NAYFEH A.H., 1990, Prediction of Bifurcations in a Parametrically Excited Duffing Oscillators, *Int. Journal Non-Linear Mechanics*, **25**, 2/3, 163-176
10. STEEB W.H., KUNICK A., 1987, Chaos in Limit Cycle Systems with External Periodic Excitations, *Int. J. Non-Linear Mechanics*, 349-361
11. SZABELSKI K., WARMIŃSKI J., 1995a, The Parametric Self Excited Non-Linear System Vibrations Analysis with the Inertial Excitation, *Int. Journal of Non-Linear Mechanics*, **30**, 2, 179-189
12. SZABELSKI K., WARMIŃSKI J., 1995b, The Self-Excited System Vibrations with the Parametric and External Excitations, *Journal of Sound and Vibration*, **187**, 4, 595-607
13. TONDL A., 1978, *On the Interaction Between Self-Excited and Parametric Vibrations*, National Research Institute for Machine Design, Monographs and Memoranda, No. 25, Prague
14. YANO S., 1989, Considerations on Self-And Parametrically Excited Vibrational Systems, *Ingenieur-Archiv*, **59**, 285-295

## Zjawiska synchronizacji i chaos w oscylatorze van der Pola-Mathieu

### Streszczenie

W pracy przedstawiono efekty oddziaływania drgań parametrycznych i samowzbudnych w układzie o jednym stopniu swobody. Analizę przeprowadzono dla nieliniowego oscylatora z samowzbudzeniem typu van der Pola oraz wzbudzeniem parametrycznym typu Mathieu, biorąc pod uwagę zarówno drgania regularne, jak i chaotyczne. Określono obszary synchronizacji drgań w otoczeniu głównego rezonansu parametrycznego oraz wyznaczono warunki, w których następuje przejście do ruchu chaotycznego. Przedstawiono również wpływ siły zewnętrznej na drgania regularne i chaotyczne układu. Wykazano, że małe wymuszenie zewnętrzne powoduje istotne zmiany jakościowe i ilościowe w obszarze głównego rezonansu parametrycznego oraz że wymuszenie zewnętrzne powoduje eliminację drgań chaotycznych i przejście układu do ruchu regularnego.

*Manuscript received November 26, 2000; accepted for print December 27, 2000*